JAMAL HONARPAZHOUH*[1], ALI ASGHAR HASSANIPAK**,
KUMARS SEIFPANAHI SHABANI***

INTEGRATION OF STREAM SEDIMENT GEOCHEMICAL AND ASTER DATA FOR PORPHYRY COPPER DEPOSIT EXPLORATION IN KHATUN ABAD, NORTH WEST OF IRAN

INTEGRACJA GEOCHEMICZNYCH DANYCH O OSADACH DENNYCH ORAZ DANYCH POZYSKANYCH Z SYSTEMU ASTER DO POSZUKIWAŃ GEOLOGICZNYCH W REJONIE ZŁÓŻ MIEDZI PORFIRYTOWEJ W KHATUN ABAD, W PÓŁNOCNO-ZACHODNIEJ CZĘŚCI IRANU

Urumieh-Dokhtar magmatic belt is the host of large porphyry copper deposits in Iran. Khatun Abad area is located in north west part of this belt, so in this study, the stream sediment geochemical survey and hydrothermal alteration zones extracted from ASTER data were used to generation new target for future lithogeochemical survey. In this study after a brief discussion on descriptive statistics, principal component analysis (PCA) and hierarchical cluster analysis were used to compress the information to a few maps and to assist in determining multi-element associations. Then C-A fractal method was used for map classification. In order to extraction hydrothermal zones ASTER data were used. ASTER SWIR bands are most useful for the identification of alteration minerals such as Alunite, Pyrophylite, Kaolinite, Sericute and Carbonates. In this paper based on spectral analysis of ASTER SWIR data six maps of alteration zones were prepared. Geochemical study and spectral analysis of ASTER data showed that mineralization and alteration are limited to E1lb and gr lithological units and have NW-SE trends from east of Khatun Abad to Ghezeljeh-Gheshlaghi.

Keywords: Porphyry copper deposit, Stream sediment, Alteration, C-A fractal, PCA, ASTER data

Pas magmowy Urumieh-Dokhtar zawiera w sobie liczne i zasobne złoża miedzi porfirytowej zalegające na terenie Iranu. Region Khatum Abad leży w północno-zachodniej części tego pasa. W pracy zebrano dane z badań geodezyjnych osadów dennych oraz dane o zmianach hydrotermalnych pobrane z systemu ASTER, dane te wykorzystano następnie do opracowania nowych celów dla badań geochemicznych skał. Praca zawiera krótki wstęp dotyczący metod statystyki opisowej, następnie przeprowadzono główną analizę składników a także hierarchiczną analizę klastrów, uzyskane dane zostały skompresowane

*   MINING EXPLORATION, FACULTY OF MINING ENGINEERING, TEHRAN UNIVERSITY, TEHRAN, IRAN.
**   GEOCHEMICAL EXPLORATION, FACULTY OF MINING ENGINEERING, TEHRAN UNIVERSITY, TEHRAN, IRAN.
***   MINING EXPLORATION, FACULTY OF MINING, PETROLEUM AND GEOPHYSICS, SHAHROOD UNIVERSITY OF TECHNOLOGY, SHAHROOD, IRAN.
[1]   CORRESPONDING AUTHOR: E-mail: honarpajooh@yahoo.com

i przedstawione w postaci map i wykorzystane do określania wieloelementowych skojarzeń. Następnie zastosowano metodę fraktali C-A do klasyfikacji map. Strefy zmian hydrotermalnych określone zostały na podstawie danych z systemu ASTER. Pasma ASTER SWIR okazały się najbardziej użyteczne przy identyfikacji zmian w zasobach minerałów, takich jak ałunit, porfiryty, kaolinit, serycyt oraz wapienie. Na podstawie analizy widmowej danych uzyskanych z systemu ASTER SWIR wygenerowano sześć map ukazujących zmiany wielkości złóż. Badania geochemiczne oraz analiza widmowa danych z systemu ASTER wykazały, że zmiany geologiczne i mineralizacja ograniczone są do strefy określonej jako E11b i wykazują tendencję do ułożenia z północnego zachodu w kierunku południowego wschodu od strony wschodniej regionu Khatum Abad do Ghezeljeh- Gheshlaghi.

Słowa kluczowe: złoża miedzi porfirytowe, osady denne, obszary zmian, fraktal C-A, dane z systemu ASTER

1. Introduction

Nowadays, geochemical exploration as an important and helpful tool was used in many aspects of studies by researchers (Gent et al., 2011; Olivella et al., 2011), in particular for investigation of stream sediments geochemistry (Carranza, 2010a, 2010b, 2011). Mineral exploration has four phases such as (1) Area selection, (2) Target generation, (3) Reserve evaluation and (4) Reserve definition (Carranza, 2009). Area selection defines permissive regions were favorable for mineral deposit formation. Target generation (purpose of this study) is an activity from regional-scale to local-scale. Target generation involves collection, analysis and integration of various thematic geosciences data sets to extract geological, geochemical and geophysical anomalies associated with mineral deposits of the type sought (Singer, 1993). Stream sediment explorations for prospecting the probable anomalies of different elements were reported in many researches (such as Nude & Arhin, 2009; Oyarzun et al., 2011; Yousefi et al., 2012). Porphyry copper deposits have large anomalies in their secondary geochemical halos and hydrothermal alteration halos as geological anomalies are wide (Yang et al., 2011). In this paper in the Khatun Abad area that itself was selected by integration of geological, geochemical and geophysical data sets, also the stream sediment geochemical anomalies and hydrothermal alteration zoning extracted from ASTER data were used to define targets for porphyry copper deposits exploration. Also, this paper is organized in five main parts. In first part the geology of Khatun Abad area is described. Subsequently geochemical study is discussed and then hydrothermal alteration zoning extraction from ASTER data discussed. Then combination of two type of extracted information is present. Finally favorable targets are promised and the results are argued.

1.1. Geological and Petrological studies of Khatun Abad area

The Khatun Abad area is situated about 45 km west of Mianeh in NW of Iran. This area is located in main Iranian belt named Urumieh-Dokhtar (Stöcklin, 1968) (see Fig. 1). The Urumieh-Dokhtar magmatic assemblage is a linear intrusive-extrusive complex with width over 4 km and extends from NW to SE Iran (Alavi, 2004). This magmatic belt has been interpreted to be a subduction related Andean-type magmatic arc that has been active from the late Jurassic to the present (Berberian & King, 1981). The northwestern part of the Urumieh-Dkhtar magmatic arc is the product of Tethys oceanic plate subducted under the Iranian microplate followed by continent-to-continent collision of the Arabian and Eurasian plates (Regard et al., 2004). Urumieh-Dokhtar
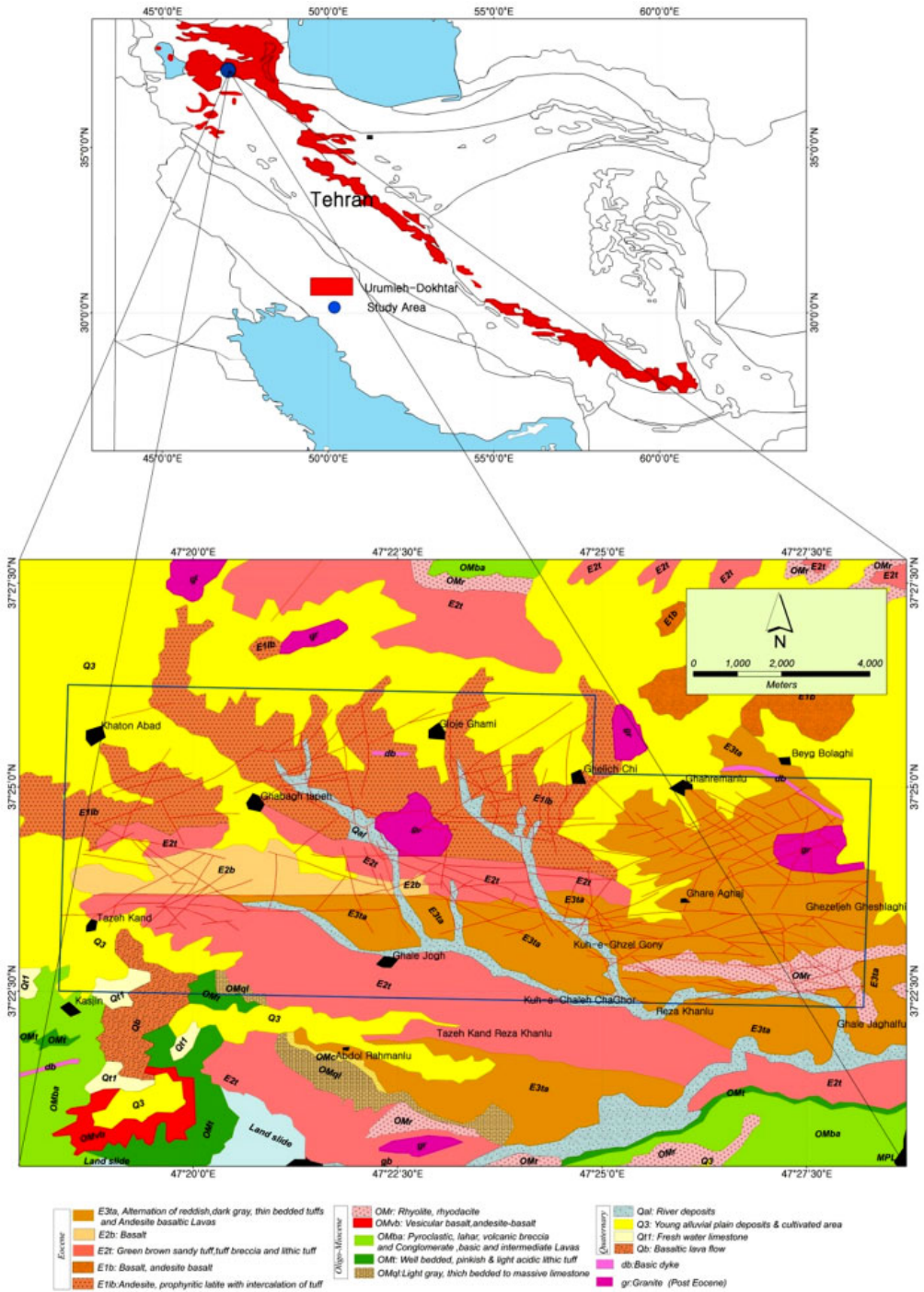
Fig. 1. Geology Map of Khatun Abad Area and its location in Urumieh-Dokhtar magmatic belt

belt is the host of large porphyry copper deposits such as Sungun in NW part, Kahang and Darre Zereshk in middle part and Meiduk and Sarcheshmeh in SE part (Shahabpour, 1994). These deposits were formed by intrusion of granodiorite-diorite stocks into Upper Cretaceous-Eocene andesitic volcano-sedimentary rocks. Shahabpour (1984) determined Rb-Sr and biotite K-Ar ages for the Sarcheshmeh porphyry 12.2 + 1.2 Ma and 12.5 + 0.5 Ma respectively. Hassanzadeh (1993) reported Rb-Sr Mineral-Whole rock age for the Meiduk porphyry 12.4 + 0.5 Ma (Hassanzadeh, 1993). According to Zarasvandi et al. (2005) studies the age of Darre zereshk porphyry is about 15 Ma (Zarasvandi et al., 2005).

The metallogenic characteristics and copper occurrences of the Urumieh-Dokhtar belt have been described by many others (e.g. Shahabpour, 1999, 2005; Richards, 2003). These Studies indicate Cenozoic granitoid and volcanic bodies related to subduction played a key role in the formation of porphyry copper mineralization in Urumieh-Dokhtar belt. Porphyry mineralization accompanied the final phases of the arc magmatism in the middle Miocene (Richards, 2003). In Mianeh region, four volcanic events of Tertiary age are recognized (Lescuyer & Riou, 1976). Extensive Eocene volcanism includes alkaline lavas and rhyolites. Oligocene volcanism is characterized by fluidal rhyolites rise up and granophyres emplacement along large fractures. Lower Miocene volcanism characterized by alternating acidic (dacites and rhyodacites) and basic (andesites and basalts) lavas. Pliocene volcanism is spottily represented by a few alkaline basalts. The Khatun Abad study area is mainly covered by Eocene and Oligomiocene volcanic-pyroclastic rocks which were intruded by monzonite to monzodiorite intrusions in Oligomiocene (Fig. 1). The extrusive rocks in Khatun Abad area including tuffs and lavas are rhyolitic to basaltic in composition. The main structural feature is Tabriz-Zanjan fault trending NW-SE and Khatun Abad area is located in the north of this fault. The second main trend is N-S which is created due to strike-slip movement of Tabriz-Zanjan fault. The alteration zones including propylitic, argilic, advanced argilic, phyllic and potassic are seen in study area. Mineralization outcrops are seen as zones of stockworks that quartz, sericite and carbonates accompanish ore minerals such as chalcopyrite, pyrite, malachite and iron oxides and hydroxides.

2. Stream Sediment Geochemical Study

Stream sediment sampling is commonly used in geochemical prospecting. The chemical composition of stream sediment samples are derived from multiple sources including upstream lithological units, mineralized bodies and in some cases contamination due to various sources. In most cases, a major proportion of variation in stream sediment uni-element concentration due to upstream lithological units (background). Separation of those concentration that related to ore bodies (anomaly) from background values is critical in geochemical prospecting and to do this, several methods have been proposed by many authors (such as Backac et al., 1999; Rantitch, 2000; Gonçalves et al., 2001; Naseem et al., 2002; Albanse et al., 2007; Ji et al., 2007; Grunski et al., 2009 and Sun et al., 2009). In this paper, firstly sampling and analytical methods is explained and then after a brief description of the single element frequency and distribution, multi-element association is discussed, then anomaly separation with multifractal modeling is performed and geochemical anomaly maps are produced.

2.1. Sampling and Analysis

In summer of 2006, 489 stream sediment samples of the –60 mesh fraction from the drainage system of study area with a density of six samples per 1 km^2 on an irregular grid were collected (Fig. 2).
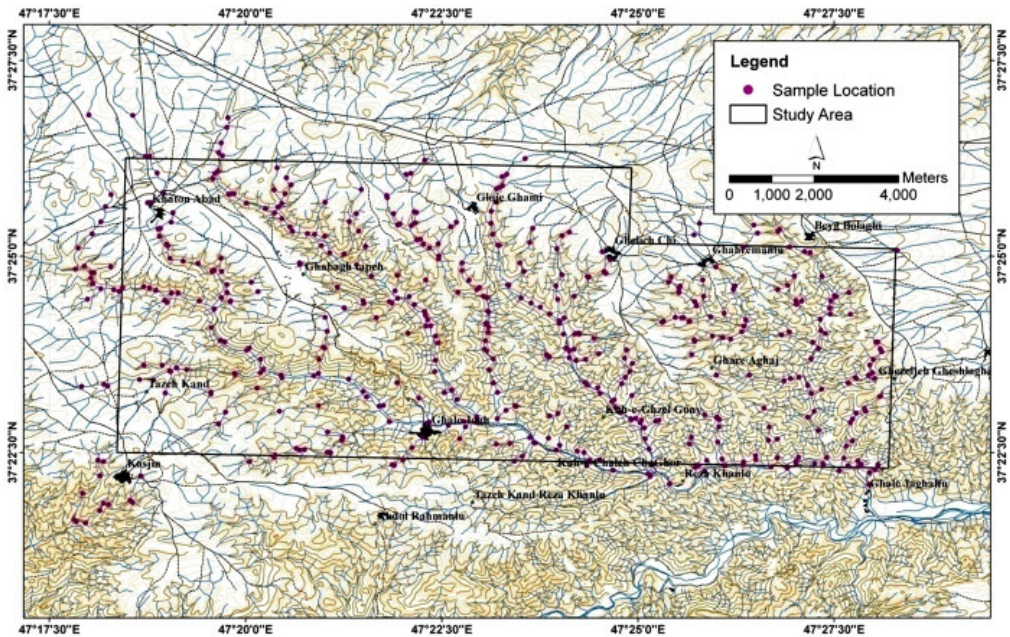

Fig. 2. Stream sediment samples location map of Khatun Abad area

Samples were collected at approximately 30 cm depth on banks or from the river bed in order to minimize the effect of seasonal climatic changes. Each sample contains the materials of at least five points in a circle with the 250 m radius and total weight of each sample was 200 gr. The sample collection protocols were described in detail by Salminen et al. (1988).

All stream sediment samples were air dried and divided into two splits using the cone and quarter method. One split was powdered to –200 mesh and sent to analyze. Analyses were carried out by Zar Azma laboratory in Iran. The Concentration of 41 major and trace elements were determined by ICP and gold was analyzed by faire assay. Data analysis was started with an appraisal of the descriptive statistics of the data. Then principal component analysis (PCA) and hierarchical cluster analysis were used to compress the information to a few maps and to assist in determining multi-element associations.

2.2. Univariate statistical methods for investigating geochemical data

Statistical parameters of 15 elements including porphyry copper deposits associated elements are presented in Table 1. Some of these elements are not the direct target of exploration but they can provide very useful pathfinders to the deposit. The frequency distribution of these elements using frequency histograms is presented in Fig. 3. As showed in Table 1 and Fig. 3 the frequency distributions of Mn and Rb elements are nearly Normal and other elements don't fol-
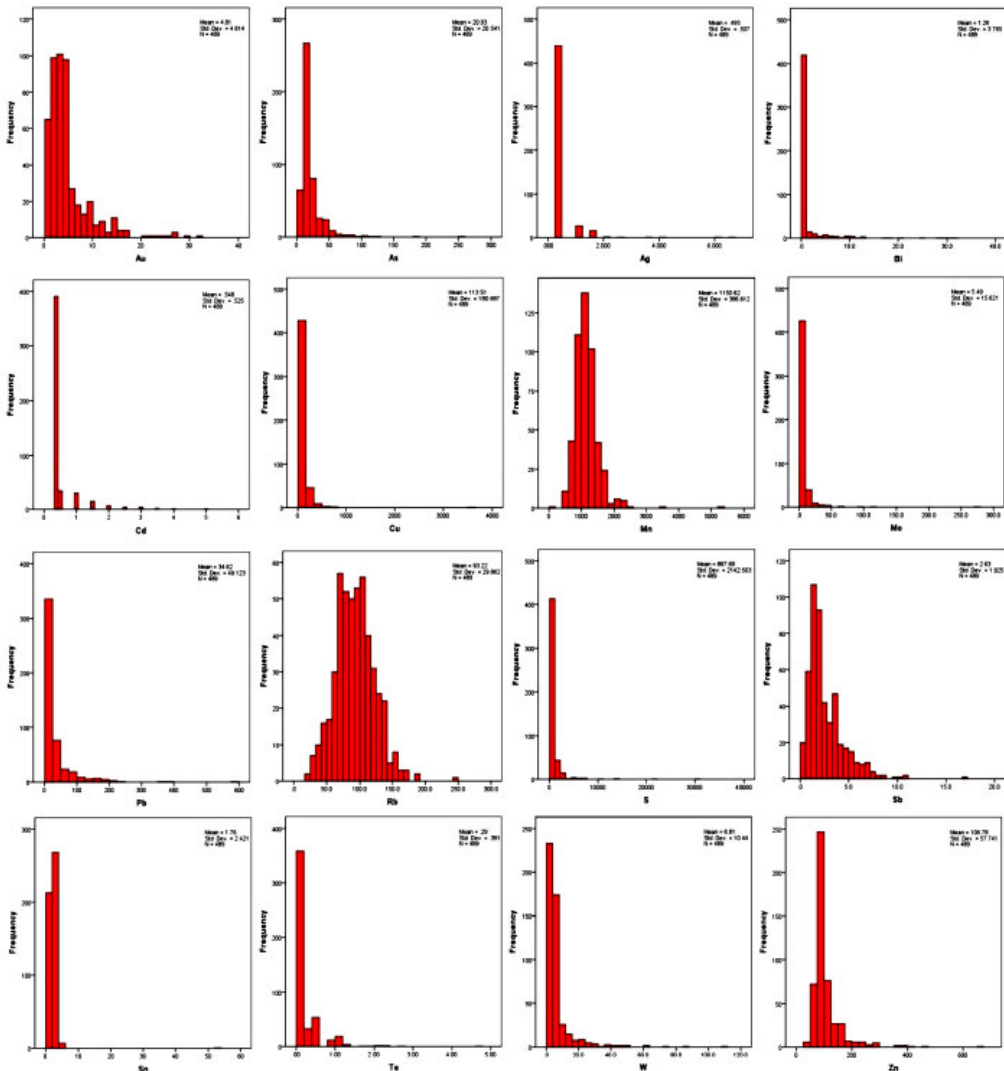

Fig. 3. Porphyry copper deposits associated elements histograms in Khatun Abad Area

low normal distribution. Table 1 show that Bi, Cu, Mo, Pb, Sb, Sn, W and Zn elements maybe have potential for mineralization.

Statistical parameters of porphyry copper deposits associated elements in Khatun Abad area

Elements	Minimum	Maximum	Mean	Std. Deviation	Skewness	Kurtosis
Ag	0.375	6.5	0.49	0.51	7.70	75.50
As	0.99	256	20.93	20.54	5.43	46.16
Au	0.75	32	4.81	4.61	2.64	8.90
Bi	0.075	31.5	1.26	3.76	5.27	32.25
Cu	22	3610	113.51	180.69	15.27	288.89
Mn	194	5210	1150.62	386.61	3.36	27.73
Mo	0.375	272	5.49	15.62	11.74	181.12
Pb	5	583	34.62	49.12	5.31	41.89
Rb	21.2	245	93.22	29.86	0.43	1.13
S	37.5	30100	887.68	2142.50	8.65	95.40
Sb	0.15	17.2	2.63	1.93	2.12	8.25
Sn	0.75	53	1.75	2.42	19.48	412.30
Te	0.15	4.8	0.29	0.39	5.42	44.23
W	0.5	109	6.81	10.44	5.05	33.41
Zn	26	666	106.78	57.74	4.09	25.38

2.3. Multivariate statistical analysis of geochemical data

Geochemical data sets are inherently multivariate. Geochemical anomalies are commonly expressed in more than one element. This is because the source or process that has generated the anomaly commonly has an association of elements. Element associations can be used to advantage by taking a multi-element approach to anomaly detection. Multi-element analysis can also identify other non ore-related associations, such as those generated by normal regolith processes or the result of anthropogenic contamination.

Table 2 represents correlation matrix of Pearson correlations coefficients of the log-transformed porphyry copper deposits associated elements in Khatun Abad area. This table shows there are relatively well correlations between these elements.

Principal component analysis (PCA) is a statistical approach for geochemical data analysis. This method can reduce the number of variables and to forming a small number of uncorrelated principal components that represent most of the variability carried by variables. In addition this method can enhance the interpretability of the components as combinations of variables (Cheng et al. 2006). In this paper the PCA has been performed on the standardized data and all of elements have been used. There were used for interpretation only the PCs whose Eigen values were higher than 1, and VARIMAX rotation was performed to best fit the variables to the axes that represent the PCs. Table 3 represents the total variance explained by first eight extracted factors and shows that by these factors 78.41% of total variability of data can be explained.

TABLE 2

Pearson correlations coefficients of the log-transformed data in Khatun Abad area

	Ag	As	Au	Bi	Cd	Cu	Mn	Mo	Pb	Rb	S	Sb	Sn	Te	W	Zn
Ag	1															
As	0.15	1														
Au	0.4	0.4	1													
Bi	0.56	0.15	0.43	1												
Cd	**0.66**	0.17	0.43	**0.75**	1											
Cu	0.55	0.21	0.48	**0.63**	**0.63**	1										
Mn	0.21	0.09	0.12	0.19	0.38	0.44	1									
Mo	0.5	0.29	0.52	**0.77**	**0.63**	**0.62**	0.2	1								
Pb	**0.66**	0.26	0.54	**0.82**	**0.81**	**0.6**	0.28	**0.7**	1							
Rb	0.3	0.44	0.45	0.33	0.28	0.41	0.13	0.51	0.47	1						
S	0.35	0.39	0.53	0.56	0.4	0.38	0.01	**0.69**	0.49	0.34	1					
Sb	0.15	0.58	0.42	0.07	0.10	0.3	0.04	0.35	0.2	**0.67**	0.3	1				
Sn	0.33	0.21	0.34	0.46	0.30	0.22	0.02	0.46	0.46	0.41	0.38	0.12	1			
Te	0.54	0.27	0.51	**0.74**	**0.73**	**0.64**	0.27	**0.7**	**0.72**	0.32	**0.63**	0.18	0.35	1		
W	0.52	0.27	0.53	**0.76**	**0.62**	**0.68**	0.22	**0.83**	**0.72**	**0.64**	0.53	0.51	0.41	**0.62**	1	
Zn	**0.6**	0.24	0.46	**0.61**	**0.79**	**0.64**	0.56	0.53	**0.78**	0.39	0.32	0.2	0.32	**0.6**	0.57	1

TABLE 3

Percentage of variance represented by all the 8 computed components in Khatun Abad area

Com-ponent	Initial Eigen values			Extraction Sums of Squared Loadings			Rotation Sums of Squared Loadings		
	Total	% of Variance	Cumula-tive %	Total	% of Variance	Cumula-tive %	**Total**	**% of Variance**	**Cumula-tive %**
1	12.5	29.7	29.7	12.5	29.7	29.7	7.9	18.9	18.9
2	6.9	16.5	46.2	6.9	16.5	46.2	6.5	15.5	34.4
3	3.9	9.3	55.5	3.9	9.3	55.5	6.0	14.3	48.7
4	3.3	8.0	63.5	3.3	8.0	63.5	4.9	11.6	60.4
5	2.4	5.7	69.1	2.4	5.7	69.1	2.5	5.9	66.2
6	1.6	3.8	72.9	1.6	3.8	72.9	1.8	4.2	70.4
7	1.2	2.9	75.8	1.2	2.9	75.8	1.7	4.0	74.5
8	1.1	2.6	78.4	1.1	2.6	78.4	1.6	3.9	78.4

Fig. 4 shows projection of variables in the three axes 1, 2 and 3 of PCA. This figure shows that five groups (consist of A-B-C-D-E) can be divided by means of these three axes.

– **Group A** , is highly correlated with component 1, reflects the association between Au, Ag, Bi, Cd, Cu, Mn, Mo, Pb, S, Te, Tl, W and Zn elements that is similar to porphyry copper deposits associated elements. Therefore anomalies of first component can be good indicators for porphyry copper mineralization in this area.
– **Group B** reflects association between Al, As, Ba, Ca, Cr, Cs, K, Li, Na, Ni, Sb, Sr and Y elements, that is strongly correlated with component 1 and but with lower loading than grope A.

- **Group C** reflects association between Be, Ce, La, Nb, Rb, Sn, Th and U elements that is highly correlated with component 2.
- **Group D** represents association between Co, Fe, Mg, Sc and V elements.
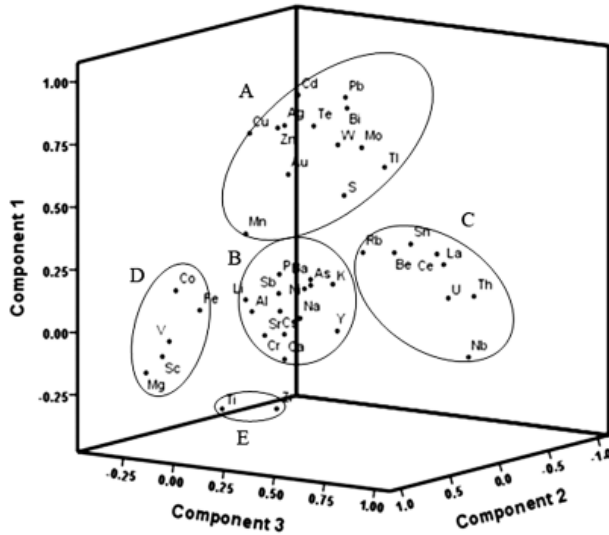- **Group E** represents association between Ti and Zr.

Fig. 4. Three dimensional scatter plot of first three components and positions of variables that were entered to PCA. This diagram shows that five groups of elements association can be divided

In order to better illustrate association between elements and to verification of PCA results, hierarchical cluster analysis (HCA) was used. Cluster analysis of variables places them into more or less homogeneous groups. Cluster analysis was performed on all elements and result is present as dendrogram in Fig. 5.

According to the dendrogram shown in Fig. 5, the 42 elements are divisible into five element groups:

- **A**: Ce, La, Nb, Sn, Th and U elements that all are lithophile elements except to Sn which is chalcophile element.
- **B**: As, Ba, Be, Cs, K, Li, Rb and Sb elements that all are lithophile elements except to As and Sb elements which are chalcophile elements.
- **C**: Ag, Au, Bi, Cd, Cu, Mo, Pb, S, Te, Tl, W and Zn elements that except to W which is lithophile element, and Au and Mo elements which are Siderophile elements. Other elements in this group are chalcophile and be possible significance for use as pathfinders for mineralization.
- **D**: Al, Co, Fe, Mg, Mn, P, Sc, Ti, V, Y and Zr elements. This group contains siderophile elements such as Co, Fe and Mn elements and lithophile elements (other elements in this group).
- **E**: Ca, Cr, Na, Ni and Sr, that all are lithophile elements except to Ni which is siderophile element.
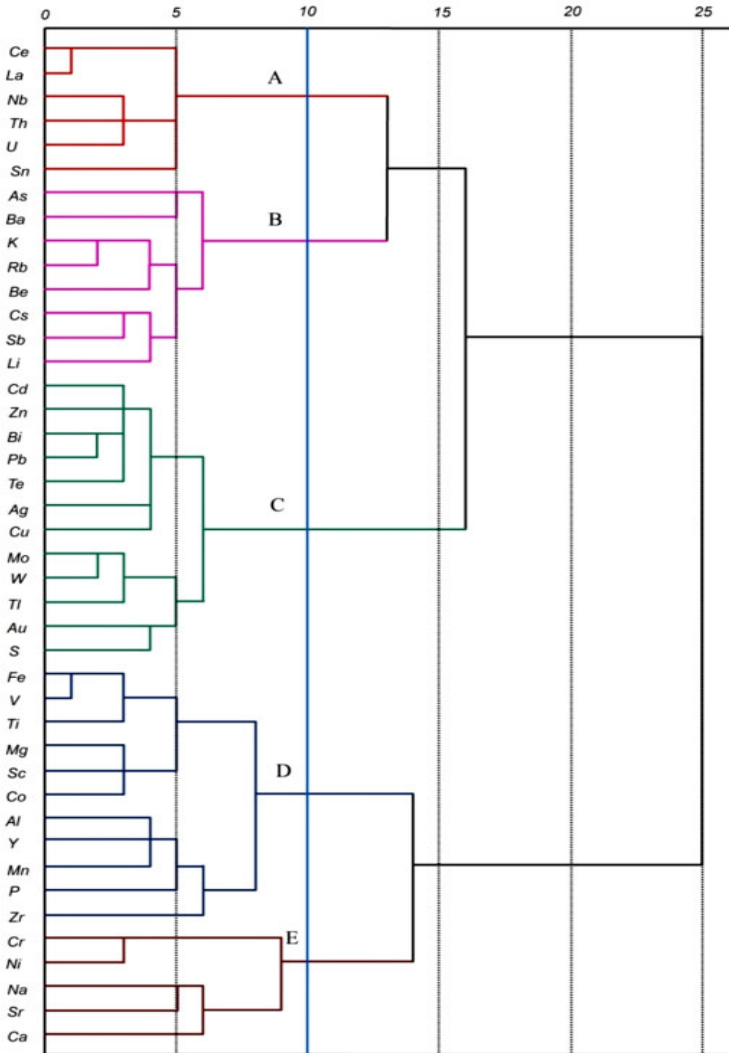
Fig. 5. Dendrogram of 42 variables from stream sediment survey in Khatun Abad area

The results of PCA and HCA in Khatun Abad area show group **A** extracted by PCA is similar to group **C** in HCA, group **C** in PCA similar to Group **A** in HCA and group **B** plus group **D** in PCA similar to group **D** in HCA. So HCA shows similar results to PCA and verifies PCA results.

2.4. Anomaly separation and Mapping

Anomaly separation plays an important role in mineral exploration. In this paper for this purpose the concentration–area model of fractal analysis was used. Cheng et al. (1994) proposed this method based on the assumption that elements distribution around ore deposits is multifractal

in nature. The concentration–area method that was proposed by Cheng et al. is based on a very simple empirical set of equations. This empirical models state that the area, $A(\rho)$, enclosing concentration values ρ lesser or equal than a pre-defined v, follow a power-law relation like:

$$A(\rho \leq v) \propto \rho^{-\alpha_1} \tag{1}$$

Conversely, for areas with concentration values ρ greater than a predefined threshold v, the relation becomes:

$$A(\rho > v) \propto \rho^{-\alpha_2} \tag{2}$$

In the equation 1 and 2, $\propto_1$ and $\propto_2$ represent characteristic exponent. Therefore, for a range of ρ values close to its minimum, the predicted multifractal power-lows take the form:

$$A(\rho) = C_1 \rho^{-\alpha_1} \tag{3-a}$$

and,

$$A(T) - A(\rho) = C\rho^{\beta} \tag{3-b}$$

where $A(T)$ is the total sampled area, C and C_1 are constants, and $\propto_1$ and β are exponents associated with the maximum singularity exponent. For the range of ρ values close to its maximum, the equation obtained is:

$$A(\rho) = C_2 \rho^{-\alpha_2} \tag{3-c}$$

Where C_2 is a constant and $\propto_2$ is the exponent associated with the maximum singularity exponent. Therefore multifractal model assumption, Equations 3-a – 3-c are equivalent to Equations 1 and 2 and whenever a plot of $\log A(\rho)$ versus $\log \rho$ is obtained, values of constants and exponents can be extracted. The break in linearity of the experimental data points occurs for the value $\rho = v$ corresponding to the threshold value for the anomalous area (Gonçalves et al., 2001).

For generation geochemical maps in Khatun Abad, the area was gridded by 100×100 m cells. Then for each variables the estimated concentration in cells were sorted out based on decreasing concentrations and cumulative areas were calculated for concentrations. Finally, Log-Log graphs for porphyry copper deposits associated elements were constructed. Fig. 6 shows this graphs for Au, Cu, Mo, Pb, W, Zn elements and first component extracted by PCA.

Breaks between straight-line trends or slope changing and the corresponding concentration in these graphs have been used as cut-offs to reclassify cell values to generate maps of distribution for desired variables (Fig. 7). According to these maps, anomalous areas are located on E1lb and gr lithological unites. E1lb is a volcanic unit which includes of andesite, porphyritic latite with intercalation of tuffs and gr is granitic intrusive body.

3. Hydrothermal Alterations extraction from ASTER data

Remote sensing images are used for mineral exploration in two applications: (1) map geology and the faults and fractures that localize ore deposits; (2) recognize hydrothermally altered rocks by their spectral signatures (Sabins, 1999). Hydrothermally altered rocks have received much attention due to association with ore deposits and appropriate spectral characteristics for identification them by remote sensing (Rowan et al., 2003; Crosta et al., 2003; Galvao et al.,
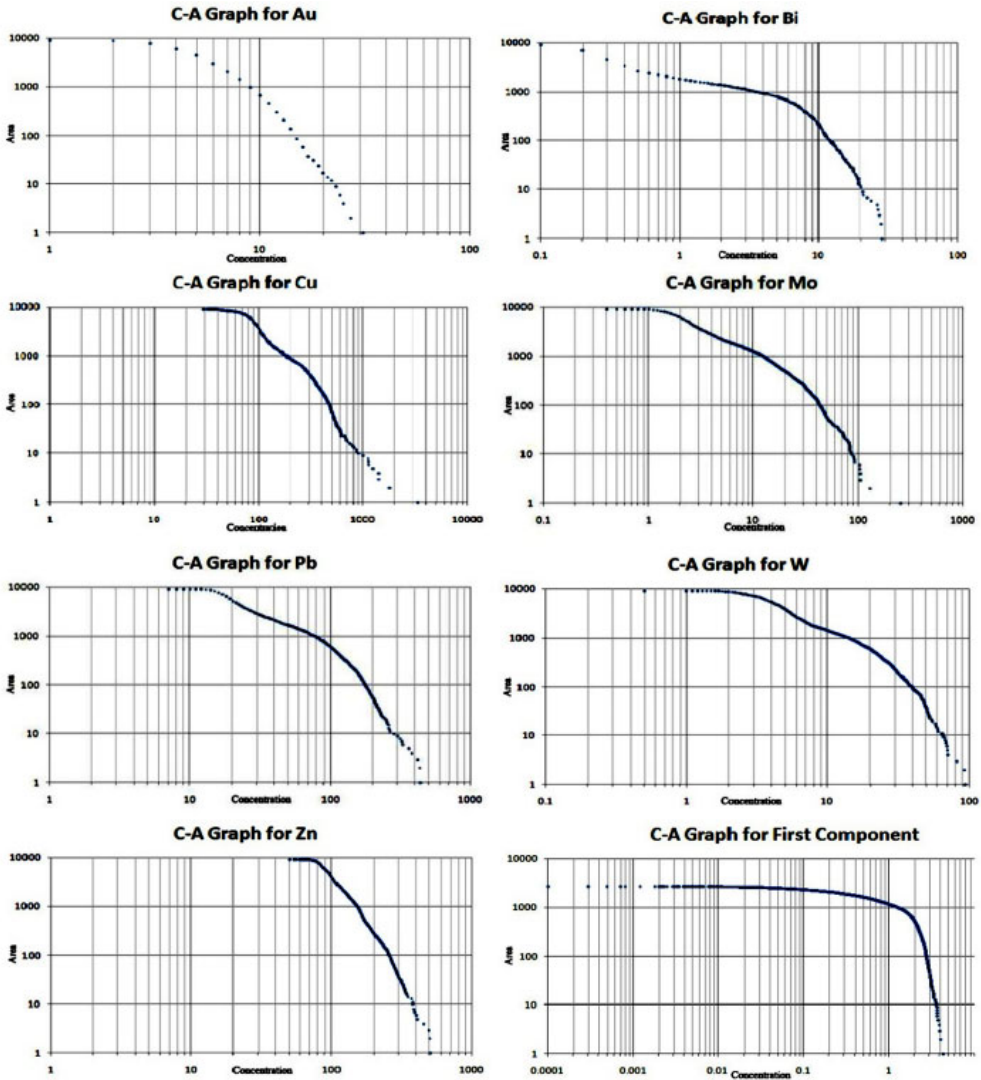
Fig. 6. Log-Log graph (C-A method) for Au, Bi, Cu, Mo, Pb, W, Zn elements and first component extracted by PCA. The vertical axis represents cumulative cell areas $A(\rho)$, with concentration values greater than ρ, and the horizontal axis is concentration values (ρ)

2005). LANDSAT and ASTER data are widely used to interpret both structure and hydrothermal alteration. One of the characteristics of ASTER data is that they have six observation bands in the SWIR (Short-Wavelength Infrared Region), particularly five bands in 2-2.4 μm region. As alteration minerals absorb rays of this region characteristically, this wavelength is most useful for the identification of alteration minerals. In LANDSAT data, this region is observed as only one band and it is difficult to identify alteration minerals by these data.
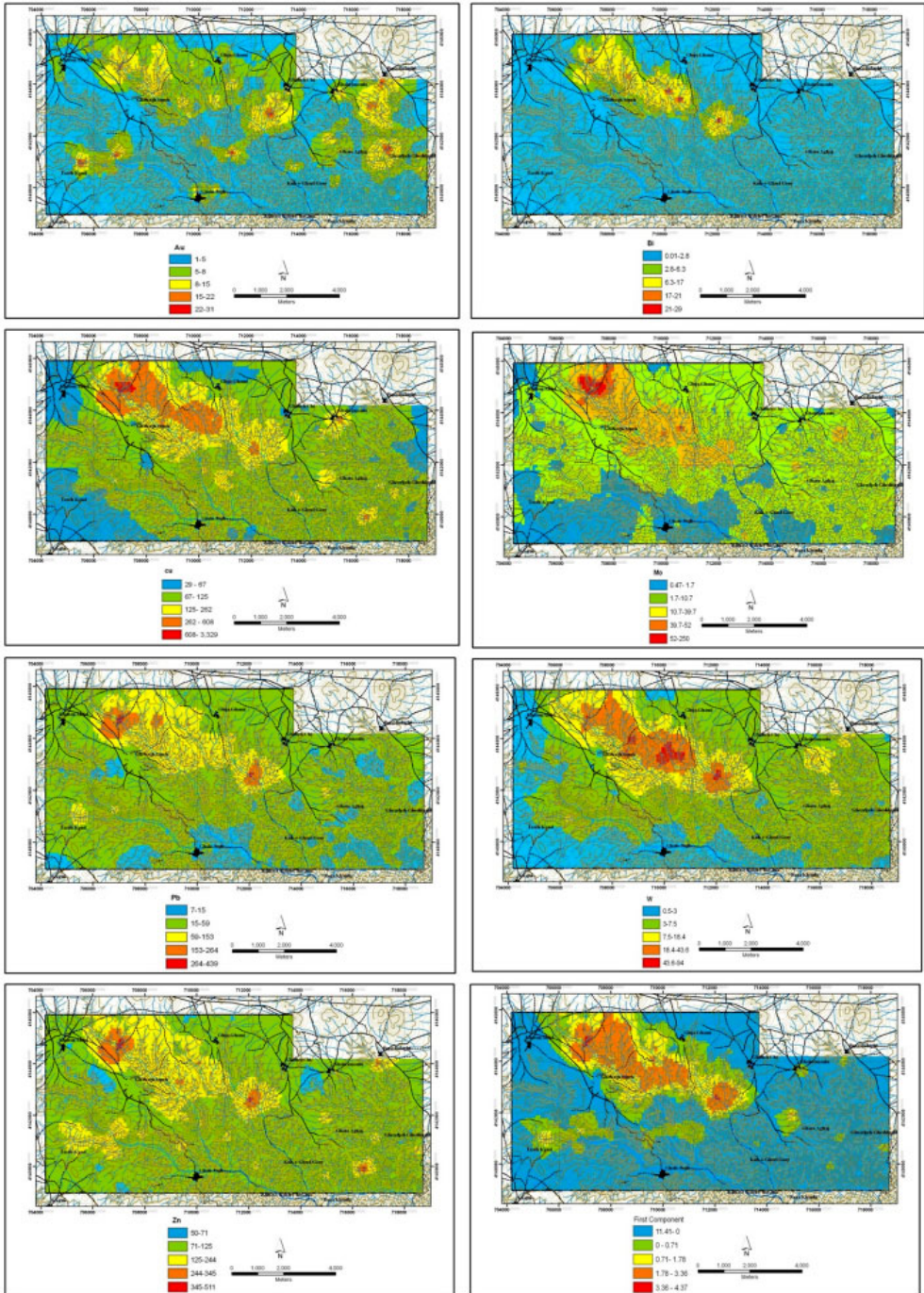
Fig. 7. Distribution maps of Au, bi, Cu, Mo, Pb, W, Zn elements and first component extracted by PCA, Classified based on C-A fractal method

50

In this Study data set AST_L1B_140700_003 in hierarchical data format (HDF) was used and for identification alteration minerals, SWIR bands (six bands) entered to processing.

Porphyry copper deposits are associated with hydrothermal alterations such as Phyllic, Potassic, Argilic and Proppylitic. Hydroxyl minerals are abundant in the phyllic, argilic and potassic zones. An oxide zone is also developed over many porphyry deposits, which is rich in iron oxide minerals (Azizi et al. 2010). The following minerals which are characteristic alteration minerals in porphyry copper deposits and epithermal vein system can be identified using the ASTER data:

    – **A**: Acid alteration minerals such as alunite, pyrophylite, kaolinite and gypsum,
    – **B**: Phyllic alteration minerals such as sericite,
    – **C**: Prophylitic alteration minerals such as chlorite, epidote and calcite,
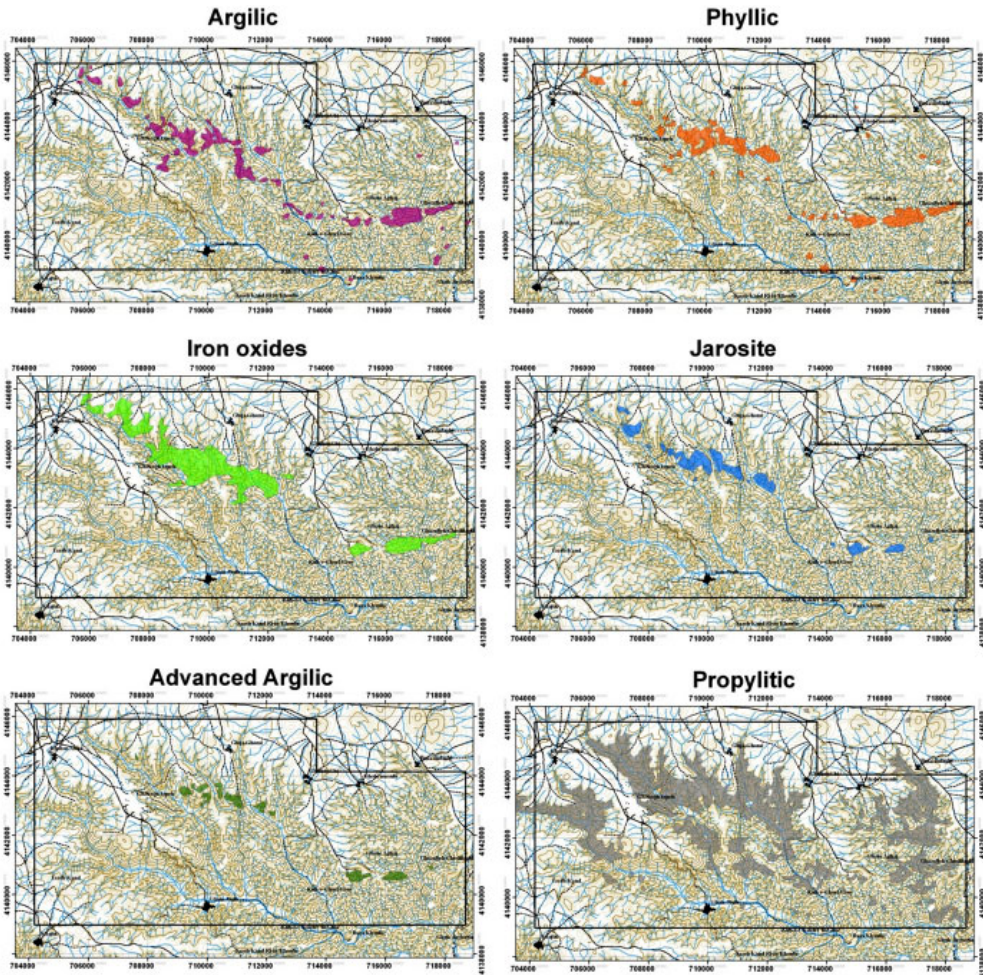   – **D**: Iron oxide minerals such as hematite, goethite and jarosite,

Fig. 8. Maps of Alteration Zones extracted from ASTER data in Khatun Abad area

In this study hydrothermal alteration extractions from ASTER data was performed in two stage, including preprocessing and mineral identification and create mineral distribution maps stages. At the first stage to remove the atmospheric and topographic effects from ASTER data, the log-residual method was used (Green and Criag, 1985). This method reduces noise from topography, instruments and sun illumination. Many processing techniques can be used to interpret the spectral data such as Band ratios; false color composite, principal component and minimum noise fraction (MNF) are important techniques that are used for the determination of alteration zones. In this paper false color composite, band ratio and minimum noise fraction are used and zones with different alteration type were determined and simplified as alteration maps in Fig. 8. This figure shows that all of altered regions are located in a belt with NW to SE trending that begins in NE Khatun Abad village and terminates in Ghezeljeh Gheshlaghi village. Alteration zones are located on E1lb, gr and E3ta lithological units. E3ta is volcano-sedimentary unit which consists of acidic grey tuff, sandy tuff, Andesitic basalt with nummulitic limestone.

4. Conclusions

Stream sediment geochemical survey and hydrothermal alteration extracted from ASTER data show the high potential for existence porphyry copper deposits in Khatun Abad area at NW of Iran. Geochemical anomalies of porphyry copper related elements which are separated by C-A fractal method have good correlation with hydrothermal alteration zones extracted from

Fig. 9. Promissed areas for lithogeochemical survey based on stream sediment survey and hydrothermal alteration zones extracted from ASTER data in Khatun Abad area, NW of Iran

ASTER data. In addition PCA shows good performance for displaying porphyry copper deposit association in this area and first component can be indicator for this type of mineralization. This study shows that mineralization in Khatun Abad limited to E1lb and gr lithological unites. E1lb is an Eocene volcanic unit which includes of andesite, porphyritic latite with intercalation of tuffs and gr is oligomicene granitic intrusive body. Apparently, mineralization is due to intrusion of this granitic body into E1lb unit. The age of mineralization in this area is consistent with metallogenetic characteristics of porphyry copper mineralization in Urumieh-Dokhtar magmatic belt that indicates porphyry mineralization accompanied the final phases of the arc magmatism in the middle miocene (Richards, 2003).

Based on this study two region (Fig. 9) were offered to National Iranian Copper Industries Company (NICICO) for more study and these regions were covered by lithogeochemical study. The results of lithogeochemical study will be published in our next paper.

Acknowledgments

References

Alavi M., 2004. *Regional Stratigraphy of the Zagros Folded-Thrust belt of Iran and its Proforeland evolution*. American Journal of Science, 304, 1-20.

Albance S., De Vivo B., Lima A., Cicchella D., 2007. *Geochemical background and baseline values of toxic elements in stream sediments of campania region (Italy)*. Journal of Geochemical Exploration, 93, 21-34.

Azizi H., Tarverdi M.A., Akbarpour A., 2010. *Extraction of hydrothermal alteration from ASTER SWIR data from east Zanjan, Northern Iran*. Advances in Space Research, 46, 99-109.

Backac M., Kumru M.N., Bassari A., 1999. *R-Mod Factor analysis applied to the exploration of radioactivity in the Gediz river*. Journal of Asian Earth Science, 19, 61-76.

Berberian M., King G.C.P., 1981. *Towards a Paleogeography and Tectonic evolution of Iran*. Canadian Journal of Earth Sciences, 18, 210-265.

Carranza E.J.M., 2009. *Geochemical Anomaly and Mineral Prospectivity Mapping in Gis*. (M. Hale, Ed.) Amsterdam, Netherlands: Elsevier. 347 pages.

Carranza E.J.M., 2010a. *Mapping of anomalies in continuous and discrete fields of stream sediment geochemical landscapes*. Geochemistry: Exploration, Environment, Analysis, 10, 171-187.

Carranza E.J.M., 2010b. *Catchment basin modelling of stream sediment anomalies revisited: incorporation of EDA and fractal analysis*. Geochemistry: Exploration, Environment, Analysis, 10, 365-381.

Carranza E.J.M., 2011. *Analysis and mapping of geochemical anomalies using logratio-transformed stream sediment data with censored values*. Journal of Geochemical Exploration, 110, 167-185.

Cheng Q., Agterberg F.P., Ballantyne S.B., 1994. *The Separation of geochemical anomalies from background by fractal methods*. Journal of Geochemical Exploration, 51, 109-130.

Cheng Q., Jing L., Panahi A., 2006. *Principal component analysis with optimum order sample correlation*. International Journal of Remote Sensing, 27 (16), 3387-3401.

Crosta A.P., De Sousa F., Azevedo C., Brodie F., 2003. *Targeting key alteration minerals in epithermal deposits in patagonia, Argentina, using ASTER imagery and principal component analysis*. International Journal of Remote Sensing, 24, 4233-4240.

Galvao L.S., Filho R.A., Vitorello I., 2005. *Use of ASTER short-wave infrared bands for the spectral discrimination of Hydrothermally altered-materials: Central Mexico*. International Journal of Remote Sensing, 19, 1981-2000.

Gent M., Menendez M., Toraño J., Torno S., 2011. *A review of indicator minerals and sample processing methods for geochemical exploration*, Journal of Geochemical Exploration, 110 (2), 47-60.

Gonçalves M.A., Mateus A., Oliveira V., 2001. *Geochemical Anomaly Separation by multifractal modeling*. Journal of Geochemical Exploration, 72, 91-114.

Green A.A., Criag M.D., 1985. Analysis *of aircraft spectrometer data with logarithmic residuals*, in Vane, G., Goetz, A. (Eds). Proceedings of the Airborn Imaging Spectrometer Data Analysis Workshop, JPL Publication, 111-119.

Grunsky E.C., Drew L.J., Sutphin D.M., 2009. *Process recognition in multi-element soil and stream-sediment geochemical data*. Applied Geochemistry, 24, 1602-1616.

Hassanzadeh J., 1993. *Metallogenic and Tectonomagmatic events in the SE sector of the cenozoic active continental margin of Iran (Shahre babak area, Kerman province)*. Unpublished Phd thesis, University of California, Los angles, 191-204.

Ji H., Zeng D., Shi Y., Wu Y., Wu X., 2007. *Semi-hierararchical correspondence cluster analysis and regionam geochemical pattern recognition*. Journal of Geochemical Exploration, 93, 109-119.

Lescuyer J.L., Riou R., 1976. *Etude géochimique du volcanise tertiaire de la région de Mianeh (Azarbaijan, Iran)*. Géologie Alpine, 52, 85-98.

Naseem S., Sheikh S.A., Qadeeruddin M., Shirin K., 2002. *Geochemical stream sediment survey in wider valley, Balochistan, Pakistan*. Journal of Geochemical Exploration, 76, 1-12.

Nude P.M., Arhin E., 2009. *Overbank sediments as appropriate geochemical sample media in regional stream sediment surveys for gold exploration in the savannah regions of northern Ghana*. Journal of Geochemical Exploration, 103 (1), 50-56.

Olivella M.À., Solé M., Gorchs R., Lao C., De Las Heras F.X.C., 2011. *Geochemical Characterization Of A Spanish Leonardite Coal*. Archive of Mining Sciences, 56 (4), 789-804.

Oyarzun R., Lillo J., López-García J.A., Esbrí J.M., Cubas P., Llanos W., Higueras P., 2011. *The Mazarrón Pb–(Ag)–Zn mining district (SE Spain) as a source of heavy metal contamination in a semiarid realm: Geochemical data from mine wastes, soils and stream sediments*. Journal of Geochemical Exploration, 109 (1-3), 113-124.

Rantitch G., 2000. *Application of Fuzzy clusters to quantify Lithological background concentrations in stream sediment geochemistry*. Journal of Geochemical Exploration, 71, 73-82.

Regard V., Bellier O., Thomas J.C., Abbassi M.R., Mercier J., Shabanian E., Fegghi K., Soleymani S., 2004. *The accommodation of Arabia-Eurasia convergence in the Zagros-Makran transfer zone, SE Iran: a transition between collision and subduction through a young deforming system*. Tectonics, 23, TC4007, 24 pages.

Richards J., 2003., *Tectono-Magmatic precursors for geophysical data over a copper gold porphyry Cu-(Mo-Au) deposit formation*. Economic Geology, 96, 1419-1431.

Rowan L.C., Hook S.J., Arams M.J., Mars J.C., 2003. *Mapping hydrothermally rocks at the cuprite nevada using the advanced spaceborne thermal emission and reflection radiometer (ASTER), a new sateiiite-imaging system*. Economic Geolog, 98, 1019-1027.

Sabins F., 1999. *Remote sensing for mineral exploration*. Ore Geology Reviews, 14, 157-183.

Salminen R.T., 1998. *FOREGS Geochemical Mapping Field Manual, Guide 47*. Geological Survey of Finland, Espoo , 36 pages.

Shahabpour J., 1984. *Aspects of Alteration and Mineralization at the Sar-Cheshmeh copper-molybdenum deposit, Kerman, Iran*. Unpublished Phd thesis, University of Leeds. 342 pages.

Shahabpour J., 1994. *Post-Mineral breccia dyke from the Sr-cheshmeh porphyry copper deposit, Kerman, Iran*. Exploration and Mining geology, 3, 39-43.

Shahabpour J., 1999. *The role of deep structures in the distribution of some major ore deposits in Iran, NE of Zagros Thrust Zone*. Journal of Geodynamics, 28, 237-250.

Shahabpour J., 2005. *Tectonic evolution of the orogenic belt in the region located between Kerman and Neyriz.* Journal of Asian Earth sciences , 24, 405-417.

Singer D.A., 1993. *Basic Concepts in three-part quantitative assessments of undiscovered mineral resources.* Nonrenewable Resources, 2, 69-81.

Stöcklin J., 1968. *Structural history and tectonics of Iran; A review.* American Association of Petroleum Geologists, Bulletin 52, 1229-1285.

Sun X., Deng J., Gong Q., Yang L., Zhao Z., 2009. *Kohenen neural network and factor analysis based approach to geochemical data pattern recognition.* Journal of Geochemical Exploration, 103, 6-16.

Yang F., Mao J., Pirajno F., Yan Sh., Liu G., Zhou G., Zhang Zh., Liu F., Geng X., Guo Ch., 2011. *A review of the geological characteristics and geodynamic setting of Late Paleozoic porphyry copper deposits in the Junggar region, Xinjiang Uygur Autonomous Region, Northwest China.* Journal of Asian Earth Sciences, In Press, Accepted Manuscript.

Yousefi M., Kamkar Rouhani A., Carranza E.J.M., 2012. *Geochemical mineralization probability index (GMPI): a new approach to generate enhanced stream sediment geochemical evidential map for increasing probability of success in mineral potential mapping.* Journal of Geochemical Exploration, In Press, Accepted Manuscript.

Zarasvandi A., Liaghat S., Zentilli M., 2005. *Geplogy of the Darreh-Zerreshk and Ali-Abad porphyry copper deposit, central Iran. International Geology* Reviews, 47 (6), 620-646.